2023 IEEE International Conference on Acoustics, Speech, and Signal Processing Workshops (ICASSPW) | 979-8-3503-0261-5/23/$31.00 ©2023 IEEE | DOI: 10.1109/ICASSPW59220.2023.10193081

JOINT WAVEFORM & WAVEFRONT ENGINEERING FOR TERAHERTZ COMMUNICATIONS IN 6G

Duschia Bodet and Josep M. Jornet

Northeastern University
Department of Electrical and Computer Engineering
Institute for the Wireless Internet of Things
360 Huntington Avenue, Boston, MA 02115

ABSTRACT

Terahertz (THz) band communications are positioned to provide the broad available bandwidths needed to fulfill society's increasing demand for faster data rates. However, due to the relatively small wavelength of THz signals and the need for high gain (i.e., electrically large compared to the wavelength) antennas, many devices that are anticipated to implement THz communications in the future will likely be operating in the near field. Of the exciting near-field solutions for THz communications, many rely on the ability to control the propagating wavefront with a thin programmable device such as an antenna array or a metasurface. However, when using a phased array or metasurface to manipulate a broadband beam, systems suffer from the well-known beam squint effect, which results in different frequencies within the signal spectrum being focused in slightly different directions. This effect can impart a frequency-selective response on a broadband signal observed by a receiver. This paper characterizes the frequency-selective response of a reconfigurable intelligent surface (RIS) and demonstrates that considering the waveform design (i.e., modulation scheme) can help improve the performance of a RIS operating on a broadband signal.

Index Terms— Terahertz Communications, Near Field, Bessel beams, Reconfigurable Intelligent Surface, Wavefront Engineering, 6G

1. INTRODUCTION

The increasing demands for faster data rates are expected to be fulfilled by communications in the Terahertz (THz) band due to the broad available bandwidths. However, because THz signals require high gain antennas and have small wavelengths, devices that are anticipated to implement THz communications in the future will often operate in the near field [1]. Traditional approaches like beamforming are suboptimal in the near field. Recently, Bessel beams have been presented as a near-field solution to provide a high gain focal region [2]. Bessel beams are often generated by passing a Gaussian beam through a refractive axicon (also called a conical lens), which uses a true time delay to introduce a phase transformation. Axicons, however, can be bulky and do not provide the flexibility that would be required for varying situations. There are many other ways to generate Bessel beams [3], and given the promise of Reconfigurable Intelligent Surfaces (RISs) for THz [4] and 6G communications [5], RIS-generated THz Bessel beams are a likely option [2].

RISs are metasurfaces or large arrays that are able to implement phase and (in some cases) amplitude transformations on an incident signal [5]. The phase of each element of the metasurface or array can be dynamically adjusted to impart the desired phase profile on the incoming wavefront. Through this phase transformation, an RIS can generate a Bessel beam or another kind of desired beam shape, but the beam will inherit some imperfections from the RIS due to the discretized phase and the element spacing. Furthermore, RISs are narrowband devices and the phase transformation they apply will differ for different incident frequencies. Thus when using an RIS to generate a Bessel beam from a Gaussian beam carrying a modulated signal with some bandwidth, the signal spectrum may be distorted.

In this paper, we explore the broadband frequency response of RIS-generated Bessel beams and the effect this frequency response will have on a broadband signal. Although this frequency response is introduced by the RIS (a hardware component of the communication system), to the signal processor at the receiver, this frequency response from the RIS would be observed as part of the channel response. Thus we propose addressing the RIS' frequency selectivity from a signal processing perspective by choosing a multi-carrier modulation scheme. We proceed to simulate the performance of single-carrier and multi-carrier broadband signals transmitted using a RIS. The results demonstrate that changing the design of the waveform can help compensate for imperfections introduced by a RIS-generated Bessel beam.

The remainder of the paper is organized as follows. We

This work was supported by the U.S. National Science Foundation (NSF) under Grants No. CNS-1955004 and CNS-2011411.

use Sec. 2 to position this paper with respect to current similar works. In Sec. 3, we describe the model used to simulate the broadband response of the RIS in MATLAB. Next, in Sec. 4, we go on to present the frequency spectrum of the simulated RIS-generated Bessel beam and how this spectrum affects single-carrier versus multi-carrier waveforms. Finally, we provide discussions and concluding remarks in Sec. 5.

2. RELATED WORK

This paper is our attempt to begin to bridge the gap between two research challenges that have - until this point - been explored independently of each other: (1) reliable beamsteering or focusing in the THz near field, and (2) the ideal modulation for THz communication systems.

2.1. Beam Control in the THz Near Field

The first challenge is the quest for a reliable method to provide high gain to THz communications devices, especially if and when these communication systems operate in the near field. In recent years the necessity to consider near-field propagation for THz communications has become apparent. The authors of [1] explore some of the key challenges and opportunities for the THz near-field along with [6], where the authors present a channel estimation model and channel estimation technique considering near-field effects. and in [7] an analysis and potential solutions for cross far and near-field communications are discussed. A few other solutions have also been presented. The authors of [8] propose a codebook solution for beamfocusing using circular arrays. Bessel beams are proposed as a potential solution in [2] to provide a strong focus in the near field. To our knowledge, none of the works attacking the problem of beam control and focusing in THz near-field couple this challenge with the modulation scheme of the communication system, which is the second challenge we discuss in this work.

2.2. Ideal Waveform for 6G and THz Communications

The ideal waveform for 6G and THz or sub-THz communications has yet to be finalized. Numerous solutions have been suggested both for single-carrier and multi-carrier systems. In terms of single-carrier solutions, the authors of [9] present chirp modulated phase shift keying (PSK) symbols to transmit across molecular absorption lines. Hierarchical Bandwidth Modulations (HBM) are suggested for broadcast THz systems [10] to exploit the distance-dependent bandwidth of the THz channel.

As for multi-carrier schemes, in [11] the authors present Distance Aware Multi-Carrier (DAMC) Modulation, an approach to allocate frequency sub-carriers in a multi-user system according to users' available bandwidth. This work was expanded on in [12] and [13] to dynamically adjust sub-carriers to accommodate the THz channel's distance-dependent characteristics. A similar approach is shared in [14], where the authors present an orthogonal frequency division multiplexing (OFDM) scheme that evaluates sub-carriers' bandwidth, power allocation, and modulation order while considering the frequency selectivity of the channel.

Although all these modulation schemes are viable solutions for THz communications, none of the works jointly considers the wavefront and waveform design.

3. SYSTEM MODEL

To model an RIS-generated Bessel beam we design a metasurface, the phase profile of which is calculated according to

$$\phi_{axicon} = \frac{|w_0 - r| \tan(\alpha)}{\lambda_0}, \tag{1}$$

where w_0 is the waist of the incident Gaussian beam at its starting point, r is the radial distance from the origin in the x-y plane, α is the angle of the equivalent conical lens, and λ_0 is the design wavelength.

Equation 1 is a continuous function, but for a metasurface behaving like an axicon the phases will be discretized to the values that are able to be generated by the metasurface. Moreover, the physical space will be partitioned by the elements of the metasurface. We design a metasurface with a quantization step of $\pi/4$ and square elements of length $851\mu m$ spaced $400\mu m$ apart. These values correspond to reasonable dimensions for a sub-THz metasurface design [15]. The resulting phase profile is what will be imparted by the metasurface axicon (metacon) and is shown in Fig. 1a.

To generate a Bessel beam we take the metacon's phase profile and apply it to a Gaussian beam. We then use the Fresnel propagation transfer function to propagate the beam through space [16]. The resulting beam is shown in Fig. 1b. Comparing it with the ideal Bessel beam shown in Fig. 1c, we see that the amplitude of the beam is reduced in the metacon version and that the focal line experiences certain peaks periodically along the z-axis. This discretization along the z-axis corresponds to the discretization we have introduced the x and y-axes by transitioning from a continuous device (refractive axicon) to a discrete device (metasurface or array). Despite this degradation, the imperfect Bessel beam generated by the metasurface still provides a gain when compared with a Gaussian beam that has not experienced the phase transformation of the metacon as shown in Fig. 1d.

Using these simulation results we assume a 10 mm x 10 mm receiving aperture is placed at some point along the z-axis within the focal range of the Bessel beam. We then calculate the power that would be observed by this receiver centered at the given location along the z-axis. We perform this analysis for the design frequency of the metacon and then repeat it for all frequencies within a certain bandwidth to find the broadband frequency response.

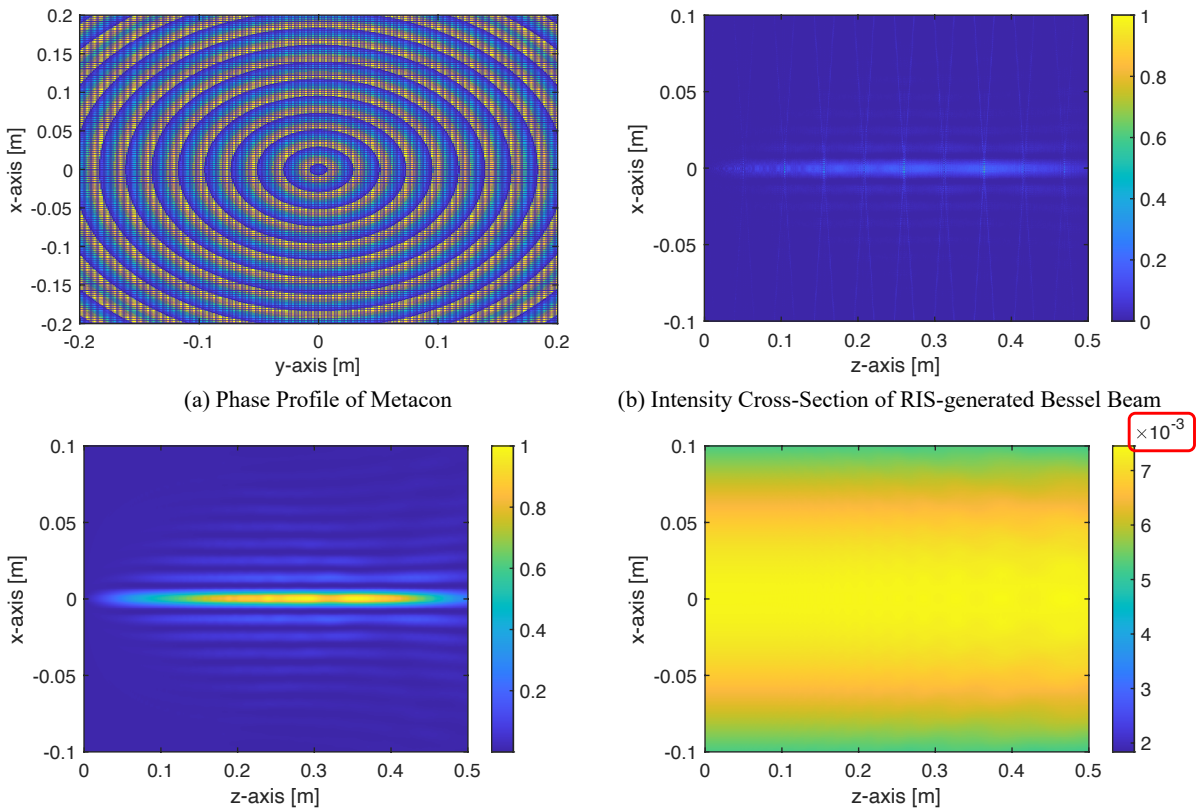

(a) Phase Profile of Metacon

(b) Intensity Cross-Section of RIS-generated Bessel Beam

(c) Intensity Cross-Section of Ideal Bessel Beam

(d) Intensity Cross-Section of Gaussian Beam

Fig. 1. Metacon Phase Profile and Performance Compared with an Ideal Bessel beam and Gaussian Beam at 130 GHz

4. RESULTS

In this section, we present our results from characterizing the frequency response of the simulated metacon and how this frequency response affects a modulated broadband signal.

4.1. Frequency Response of Bessel beam Generating Device

We explore the broadband frequency response of the ideal axicon and the metacon compared with that of a Gaussian beam that has not been manipulated. The results are plotted in Fig. 2a. It is clear that the power received in the case of an ideal axicon (shown in red) produces a close to a 6 dB gain compared with the Gaussian case as we would anticipate from the axicon design parameters. Another interesting observation is that the power increases steadily with frequency; this gradual incline is due to the fact that as the frequency increases, the Bessel beam generated by any axicon creates a thinner focal line [17] resulting in more power captured by the receiving aperture.

Similar to the cross-section shown in Fig. 1, we again see that the overall received power for the case of the metacon (shown in yellow) is lower than that of the perfect axicon due to the discretization we have added both in space and in phase. We also observe the frequency-selective nature of the RIS in the peaks and troughs shown in Fig. 2. Another observation is that the peak frequency in Fig. 2 does not necessarily correspond to the design frequency of 130 GHz. This discrepancy is a combination of the frequency-selective nature of the RIS and the fact that the beam is no longer continuous; it suffers from nulls because of the space between RIS elements. Due to the element spacing, an array or a metasurface attempting to generate a Bessel beam actually generates a series of focal points along the z-axis instead of the continuous focal line generated by a perfect axicon. We can see this in our comparison of Fig. 1b and c. Additionally, changing the frequency of the beam incident on the metacon shifts the focal points in space. Thus each frequency produces peaks at slightly different locations along the z-axis. In our case, 20 cm is not exactly at a peak for the design frequency of the RIS, but it is closer to a peak for 138 GHz. If we were to pick a different point along the z-axis to place our receiver, the frequency response of the metacon would change. For example, in Fig. 2b, we show the received power for a receiver placed at 24 cm,

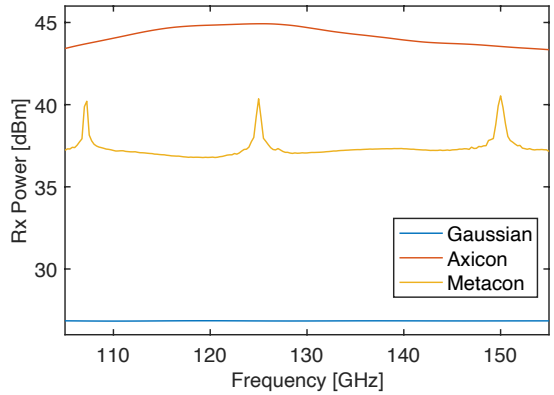

(a) Received Power at 30cm

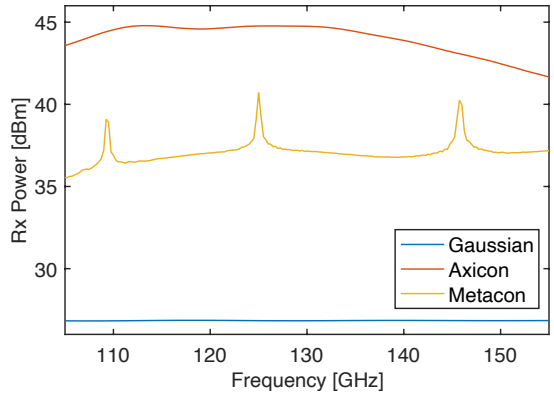

(b) Received Power at 35cm

Fig. 2. Received Power and Normalized Received Power Spectrum for a 10 mm x 10 mm receiving aperture at 20 cm

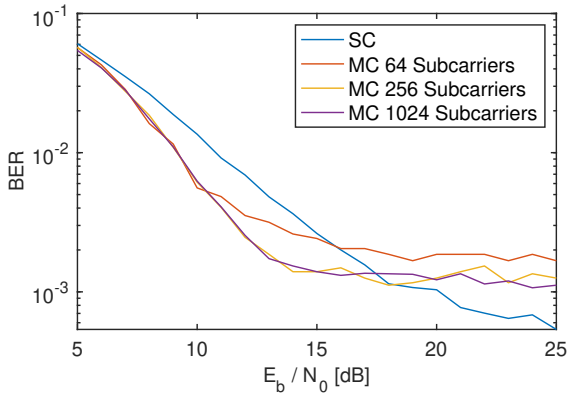

Fig. 3. Error Rate Performance of Single-Carrier (SC) vs Multi-Carrier (MC) Modulations

and the response has changed with a peak much closer to the design frequency at 130 GHz.

Despite these imperfections introduced by the RIS, the metacon still provides a gain compared to the regular Gaussian beam case, and therefore it still provides the benefits of higher gain for near-field THz communications as proposed in [2]. The frequency selectivity of the device, however, will impact the communication system performance.

4.2. Performance Analysis of Single-Carrier vs. Multi-Carrier Modulations with Metacon

To evaluate the impact that this frequency-selectivity will have on a transmitted broadband signal, we proceed to apply the frequency response shown in Fig. 2a to a broadband modulated signal. We have simulated single-carrier and multi-carrier waveforms centered at 130 GHz and modulated using 16-QAM with a bandwidth of 50 GHz. After adding noise and applying the frequency responses, we demodulate and detect the received bits for various energy per bit noise ratios. The resulting bit error rates (BERs) are shown as a function of the energy per bit noise ratio in Fig. 3. For the multi-carrier schemes, we notice that as the number of subcarriers increases the BER performance improves. Adittionally, the single-carrier performance is notably worse than the multi-carrier schemes for low E_b/N_0 scenarios, but as the E_b/N_0 increases, the single-carrier scheme begins to outperform the multi-carrier schemes.

From these findings we demonstrate that although single-carrier modulation schemes have traditionally been favored for THz communications due to their low peak-to-average power ratios (PAPRs), multi-carrier schemes can provide improved performance in some cases. Particularly, in this scenario, the partitioning of the frequency band into sub-bands for each carrier improves the error rate performance of information-bearing RIS-generated beams for low SNR or E_b/N_0 scenarios.

5. CONCLUSIONS AND FUTURE DIRECTIONS

In this work, we demonstrate that due to the frequency-selective nature of RISs, the waveform used for broadband communications should be carefully considered. While the ideal waveform for 6G has yet to be finalized, in many works, the simplicity of a single-carrier scheme is favored. The reality, however, is that multi-carrier communications can come in handy not just for spectral efficiency but also to adjust for frequency-selective hardware components. Although for this analysis we only implement OFDM and do not adjust the power allocated to certain subcarriers or change the modulation scheme used on those subcarriers, those approaches could be implemented to further enhance multi-carrier schemes' ability to compensate for RISs' frequency-selectivity. Multi-carrier schemes still have their challenges for THz systems (such as high PAPRs) and therefore methods to optimize the system performance considering both the wavefront and waveform design simultaneously must be considered in future work.

6. REFERENCES

[1] M. Cui, Z. Wu, Y. Lu, X. Wei, and L. Dai, "Near-field communications for 6g: Fundamentals, challenges, potentials, and future directions," *arXiv preprint arXiv:2203.16318*, 2022.

[2] A. Singh, A. J. Alqaraghuli, and J. M. Jornet, "Wavefront engineering at terahertz frequencies through intelligent reflecting surfaces," in *2022 IEEE 23rd International Workshop on Signal Processing Advances in Wireless Communication (SPAWC)*. IEEE, 2022, pp. 1–5.

[3] S. N. Khonina, N. L. Kazanskiy, P. A. Khorin, and M. A. Butt, "Modern types of axicons: New functions and applications," *Sensors*, vol. 21, no. 19, p. 6690, 2021.

[4] F. Yang, P. Pitchappa, and N. Wang, "Terahertz reconfigurable intelligent surfaces (riss) for 6g communication links," *Micromachines*, vol. 13, no. 2, p. 285, 2022.

[5] Y. Liu, X. Liu, X. Mu, T. Hou, J. Xu, M. Di Renzo, and N. Al-Dhahir, "Reconfigurable intelligent surfaces: Principles and opportunities," *IEEE communications surveys & tutorials*, vol. 23, no. 3, pp. 1546–1577, 2021.

[6] A. M. Elbir, W. Shi, A. K. Papazafeiropoulos, P. Kourtessis, and S. Chatzinotas, "Near-field terahertz communications: Model-based and model-free channel estimation," *IEEE Access*, 2023.

[7] C. Han, Y. Chen, L. Yan, Z. Chen, and L. Dai, "Cross far-and near-field wireless communications in terahertz ultra-large antenna array systems," *arXiv preprint arXiv:2301.03035*, 2023.

[8] Y. Xie, B. Ning, L. Li, and Z. Chen, "Near-field beam training in thz communications: The merits of uniform circular array," *IEEE Wireless Communications Letters*, 2023.

[9] P. Sen, H. Pandey, and J. M. Jornet, "Ultra-broadband chirp spread spectrum communication in the terahertz band," in *Next-Generation Spectroscopic Technologies XIII*, vol. 11390. SPIE, 2020, pp. 7–18.

[10] D. Bodet, P. Sen, Z. Hossain, N. Thawdar, and J. M. Jornet, "Hierarchical bandwidth modulations for ultra-broadband communications in the terahertz band," *IEEE Transactions on Wireless Communications*, 2022.

[11] C. Han, A. O. Bicen, and I. F. Akyildiz, "Multi-wideband waveform design for distance-adaptive wireless communications in the terahertz band," *IEEE Transactions on Signal Processing*, vol. 64, no. 4, pp. 910–922, 2015.

[12] C. Lin and G. Y. Li, "Adaptive beamforming with resource allocation for distance-aware multi-user indoor terahertz communications," *IEEE Transactions on Communications*, vol. 63, no. 8, pp. 2985–2995, 2015.

[13] A. Shafie, N. Yang, S. A. Alvi, C. Han, S. Durrani, and J. M. Jornet, "Spectrum allocation with adaptive sub-band bandwidth for terahertz communication systems," *IEEE Transactions on Communications*, vol. 70, no. 2, pp. 1407–1422, 2021.

[14] A.-A. A. Boulogeorgos, E. N. Papasotiriou, and A. Alexiou, "A distance and bandwidth dependent adaptive modulation scheme for thz communications," in *2018 IEEE 19th International Workshop on Signal Processing Advances in Wireless Communications (SPAWC)*. IEEE, 2018, pp. 1–5.

[15] H. Guerboukha, Y. Amarasinghe, R. Shrestha, A. Pizzuto, and D. M. Mittleman, "High-volume rapid prototyping technique for terahertz metallic metasurfaces," *Optics Express*, vol. 29, no. 9, pp. 13 806–13 814, 2021.

[16] D. G. Voelz, *Computational fourier optics: a MATLAB tutorial*. SPIE press Bellingham, Washington, 2011, vol. 534.

[17] M. S. Kulya, V. A. Semenova, V. G. Bespalov, and N. V. Petrov, "On terahertz pulsed broadband gauss-bessel beam free-space propagation," *Scientific reports*, vol. 8, no. 1, pp. 1–11, 2018.